THE JOURNAL OF BIOLOGICAL CHEMISTRY VOL. 290, NO. 30, pp. 18732–18743, July 24, 2015

Tryptophan Scanning Mutagenesis Identifies the Molecular Determinants of Distinct Barttin Functions*

Received for publication, December 19, 2014, and in revised form, May 13, 2015 Published, JBC Papers in Press, June 10, 2015, DOI 10.1074/jbc.M114.625376

Daniel Wojciechowski[‡], **Martin Fischer**[‡], **and Christoph Fahlke**[§1]

From the [‡]*Institut für Neurophysiologie, Medizinische Hochschule Hannover, 30625 Hannover, Germany and* [§]*Institute of Complex Systems-Zelluläre Biophysik (ICS-4), Forschungszentrum Jülich, 52428 Jülich Germany*

Background: Barttin is an accessory subunit of renal and inner ear chloride channels.
Results: Tryptophan insertion at multiple barttin residues results in non-functional CLC-K/barttin channels with normal intracellular trafficking.
Conclusion: Gating of CLC-K/barttin channels is more sensitive to tryptophan insertion in barttin than intracellular trafficking.
Significance: Understanding the molecular basis of CLC-K modification by its accessory subunit barttin.

CLC-K chloride channels are expressed in the kidney and in the inner ear and require the accessory subunit barttin for proper function and membrane insertion. Barttin exerts multiple functions on CLC-proteins: it modifies protein stability and intracellular trafficking as well as channel activity, ion conduction, and gating. So far, the molecular determinants of these distinct barttin functions have remained elusive. Here we performed serial perturbation mutagenesis to identify the sequence determinants of barttin function. Barttin consists of two transmembrane helices followed by a long intracellular carboxyl terminus, and earlier work demonstrated that the transmembrane core of barttin suffices for most effects on the α-subunit. We individually substituted every amino acid of the predicted transmembrane core (amino acids 9–26 and 35–55) with tryptophan, co-expressed mutant barttin with hClC-Ka or V166E rClC-K1, and characterized CLC-K/barttin channels by patch clamp techniques, biochemistry, and confocal microscopy. The majority of mutations left the chaperone function of barttin, *i.e.* the effects on endoplasmic reticulum exit and surface membrane insertion, unaffected. In contrast, tryptophan insertion at multiple positions resulted in impaired activity of hClC-Ka/barttin and changes in gating of V166E rClC-K1/barttin. These results demonstrate that mutations in a cluster of hydrophobic residues within transmembrane domain 1 affect barttin-CLC-K interaction and impair gating modification by the accessory subunit. Whereas tight interaction is necessary for functional modification, even impaired association of barttin and CLC-K suffices for normal intracellular trafficking. Our findings allow definition of a likely interaction surface and clarify the mechanisms underlying CLC-K channel modification by barttin.

CLC-K channels are members of the CLC family of voltage-gated chloride channels and transporters that are exclusively expressed in epithelial cells (1). Distinct CLC-K channels have been identified from rat (rClC-K1 and rClC-K2) (2, 3), mouse (mClC-K1 and mClC-K2) (4), and humans (hClC-Ka and hClC-Kb) (5) and have been shown to be essential for sensory transduction in the inner ear and for normal urinary concentration. They mediate Cl^- efflux in the thin ascending limb (ClC-K1/ClC-Ka; Refs. 6 and 7) and in the thick ascending limb of Henle's loop (ClC-K2/ClC-Kb; Ref. 8) necessary for the countercurrent multiplier mechanism and extracellular NaCl and urea accumulation in the renal medulla. In the stria vascularis of the inner ear, both isoforms cooperate in mediating basolateral Cl^- efflux and secondary active K^+ secretion into the endolymph by marginal cells (9).

When expressed alone in *Xenopus* oocytes or mammalian cells, neither hClC-Ka nor hClC-Kb/K2 forms functional channels (5). Co-expression of CLC-K with barttin, the product of the disease gene *BSND* of Bartter syndrome IV (10), results in the occurrence of functional channels (11–14). Barttin acts as an accessory subunit that stabilizes the CLC-K protein and promotes its insertion into the plasma membrane (11–15). Moreover, barttin switches human CLC-K channels from a non-conductive into an active conformation (14, 16, 17). Whereas the transmembrane core of barttin is sufficient for fulfilling the effects on channel stability and intracellular trafficking, additional amino acids in the carboxyl terminus are required for normal function of CLC-K/barttin channels (14, 17).

The molecular determinants of these different functions of barttin are insufficiently understood. The functional analysis of disease-associated mutations found in patients with Bartter syndrome IV revealed that many mutations did not modify the different functions of barttin in a similar way. Some abolished hClC-Ka/barttin and hClC-Kb/barttin functions but left intracellular CLC-K/barttin trafficking unaltered (15), whereas another one exclusively impaired surface membrane insertion (18). To identify amino acids crucial for the different functions of barttin, we individually substituted each residue within the predicted transmembrane core of barttin by tryptophan (19–24) and studied the effects of these mutations by heterologous expression and functional as well as biochemical analyses. Using this approach we identified residues important for the stability of barttin or for its intracellular trafficking and functional interaction with CLC-K channels.

* This work was supported by the Deutsche Forschungsgemeinschaft (FA301/10; to Ch. F). The authors declare that they have no conflicts of interest with the contents of this article.
[1] To whom correspondence should be addressed. E-mail: c.fahlke@fz-juelich.de.

Experimental Procedures

Mutagenesis and Heterologous Expression—To express tryptophan-substituted mutant barttin, point mutations were introduced into a pcDNA3.1(+) expression construct encoding a WT barttin-mCFP fusion protein (14) using the QuikChange site-directed mutagenesis kit (Agilent Technologies, Santa Clara, CA).

To study the effects of mutant barttin on intracellular trafficking or on channel expression and function we used heterologous expression in two different cell lines, MDCKII and HEK293T cells (14–16, 18). CLC-K/barttin function and subcellular distribution are comparable in both systems (14, 25). However, higher expression levels make HEK293T cells less suited for studying intracellular distribution as MDCKII cells. In contrast, robust expression in HEK293T cells permits even functional characterization of channel mutants with significant alterations in function or cellular distribution.

For biochemical experiments or confocal imaging approaches HEK293T (barttin expression) or MDCKII cells (glycosylation of CLC-K, surface insertion of barttin or CLC-K) were transfected either with 2 μg of pcDNA3.1(+) barttin-mCFP alone or together with 1 μg of pcDNA3.1(−) YFP-hClC-Ka using calcium phosphate precipitation (16) or Lipofectamine 2000 (Invitrogen). For electrophysiological measurements, HEK293T cells were transiently co-transfected with 4 μg pcDNA3.1(+) barttin-mCFP together with 2 μg of pcDNA3.1(−) YFP-hClC-Ka or 1–2 μg of pRcCMV YFP-V166E rClC-K1 using calcium phosphate precipitation (16). We usually transfected 2–4-fold larger DNA amounts of barttin-encoding plasmids to ensure overabundant barttin expression and saturation of all barttin binding sites within the CLC-K proteins.

Electrophysiological experiments were performed typically one (hClC-Ka) or two days (V166E rClC-K1) after transfection. Only cells for which visual inspection revealed higher mCFP (barttin) than YFP (CLC-K) fluorescence were used for electrophysiological analysis.

Confocal Microscopy—Live cell confocal imaging was performed on transiently transfected MDCKII cells on a Leica DM IRB inverted microscope with a TCS SP2 AOBS scan head in 63× magnification. Subcellular distribution of barttin-mCFP was investigated using 405-nm excitation wavelength and fluorescence detection within the range of 450–500 nm, whereas an excitation wavelength of 514 nm and fluorescence detection at 520–600 nm was used for imaging YFP-hClC-Ka channels. LCS software (Leica, Wetzlar, Germany) was used for image acquisition, and ImageJ/Fiji software (Wayne Rasband, National Institutes of Health) for image processing.

Protein Biochemistry—HEK293T or MDCKII cells were lysed by incubation in 1% Triton X-100 in the presence of protease inhibitors (Sigma, Hamburg, Germany). Cleared lysates were denatured for 15 min at room temperature in Laemmli buffer containing SDS and DTT and electrophoresed in parallel with fluorescent mass markers (Dual Color, Bio-Rad) on 12% SDS-polyacrylamide gels. Fluorescence-tagged proteins were visualized by scanning the wet PAGE gels with a fluorescence scanner (Typhoon, GE Healthcare, München, Germany). Individual bands were quantified with the ImageQuant software (GE Healthcare, München, Germany). Expression levels are given as relative values after normalization to WT protein fluorescence determined in the same series of experiments.

Surface biotinylation was performed 36–40 h after transfection by incubating MDCKII cells with 0.375 mg EZ-link Sulfo-NHS-SS-Biotin (Thermo Scientific, Rockford, IL) in 1.5 ml of PBS for 30 min as described (26). After washing with PBS and quenching with 100 mM glycine in PBS, cells were lysed, 1 mg of lysate was incubated with 150 μl of High Capacity NeutrAvidin Agarose Resin (Thermo Scientific) for at least 2 h, and biotin-labeled proteins were eluted with 100 μl of Laemmli buffer containing SDS and DTT. Cleared lysates and elution fractions were denatured at room temperature in Laemmli buffer, electrophoresed in parallel with fluorescence mass marker (Dual Color; Bio-Rad, München, Germany; Broad Range, Thermo Scientific, Darmstadt, Germany) on a 12% SDS-polyacrylamide gel and visualized using a fluorescence scanner (Typhoon, GE Healthcare). Gels were blotted on nitrocellulose membranes (Bio-Rad), developed with mouse-α-GAPDH and HRP-α-mouse IgG, and detected with SuperSignal™ West Pico Chemiluminescent Substrate (Thermo Fischer). Results were taken only from experiments in which no GAPDH was detected in purified membrane fractions and are given as relative values compared with WT barttin data that served as control in each experiment.

Electrophysiology—Standard whole-cell patch clamp recordings were performed using an Axopatch 200B amplifier (Molecular Devices, Sunnyvale, CA) as described (16, 27). Pipettes were pulled from borosilicate glass and had resistances between 1.0 and 2.2 megaohms. For noise analysis, pipettes were covered with dental wax to reduce their capacitance. More than 80% of the series resistance was compensated by an analog procedure, resulting in calculated voltage errors of <5 mV. Between test sweeps, cells were clamped to 0 mV for at least 5× the duration of one individual sweep. The standard extracellular solution contained 140 mM NaCl, 4 mM KCl, 2 mM $CaCl_2$, 1 mM $MgCl_2$, and 5 mM HEPES, pH 7.4. The standard intracellular solution contained 120 mM NaCl, 2 mM $MgCl_2$, 5 mM EGTA, 10 mM HEPES, pH 7.4. Currents were filtered at 5 kHz and digitized with a sampling rate of 20 kHz. hClC-Ka/mutant barttin channels that resulted in current amplitudes below 500 pA at +105 mV in transfected cells together with the absence of the characteristic hook-shaped I-V-plot were interpreted as non-functional. Stationary noise analysis was performed as described (18). For this purpose, currents were filtered at 10 kHz and digitized with a sampling rate of 50 kHz. The data were analyzed with a software combination of pClamp 8/9/10 (Molecular Devices) and Sigma Plot (Jandel Scientific, San Rafael, CA). Isochronal current amplitudes were measured after capacitive current relaxation, usually 0.5 ms after the voltage step. Activation curves of hClC-Ka/barttin (Fig. 3*E*) were obtained from dividing steady-state current amplitudes by the electrical driving force and two unitary channel parameters obtained from noise analysis, *i.e.* the unitary current conductance, and the number of channels (Fig. 3, *D*–*G*) (16, 18).

To obtain the relative probabilities of V166E rClC-K1/barttin channel openings, isochronal current amplitudes 0.5 ms

after stepping to −125 mV were plotted *versus* the voltage of a preceding 300–600-ms pulse (Fig. 4, *A–F*) and normalized to maximum values obtained from the Boltzmann fit. To determine the voltage dependence of the slow gate open probability in V166E rClC-K1, we inserted a short step to +180 mV (5 ms) that fully activated the fast gate (16). Fast activation curves were determined by dividing relative probabilities of channels to be open by open probabilities of the slow gate. All activation curves were fit with a modified Boltzmann equation exhibiting a voltage-independent minimum open probability (P_{min}) and a voltage-dependent term,

$$P(V) = \frac{P_{max} - P_{min}}{1 + e^{\frac{ze_0F(V - V_{0.5})}{RT}}} + P_{min} \quad \text{(Eq. 1)}$$

with ze_0 being the apparent gating charge, P_{max} the maximum open probability, and $V_{0.5}$ the midpoint of activation. For all barttin mutations, the midpoint of fast gate activation (Fig. 4*H*) and the voltage-dependent component of slow gating $\Delta p_{slow\ gate} = P_{maxslow} - P_{minslow}$ (Fig. 4*I*) were determined. All values are given as the mean ± S.E.

Results

Barttin's Chaperone Function Is Not Affected by the Majority of Single Tryptophan Substitutions—When expressed alone barttin inserts into the surface membrane of mammalian cells. In contrast, a large percentage of CLC-K channels remains in the endoplasmic reticulum in the absence of barttin. Co-expression of CLC-K and barttin results in improved insertion of CLC-K into the surface membrane, a barttin function we will refer to as chaperone function of barttin. To investigate the effects of tryptophan insertion on this particular function, we first tested whether tryptophan substitution of single amino acids of the predicted transmembrane helices TM1 or TM2 interferes with correct folding of barttin. We resolved lysates from HEK293T cells transfected with plasmids encoding WT or mutant barttin-mCFP fusion proteins by SDS-PAGE. For WT as well as for the majority of mutant barttins, a predominant band at 63 kDa was observed in such experiments. Only transfection with plasmids encoding F24W or M26W barttin resulted in the expression of proteins with lower molecular mass than WT barttin, indicating misfolding and/or degradation of the protein (Fig. 1*A*). M40W, G41W, and V45W barttin-mCFP could be detected as full-length protein but with relative expression levels below 12% of WT barttin (Fig. 1*B*; visible upon overexposure in the *lower panel*). We found six additional mutations (G35W, I46W, G47W, G48W, I49W, and S52W) that reduced expression levels significantly but moderately to ~70% (Fig. 1*C*). Because such moderate reductions still permit barttin expression in excess over CLC-K, we did not separate these mutations from those with normal expression levels. Confocal imaging of MDCKII transfected with plasmids encoding WT or mutant barttin alone demonstrated that all mutant barttins that express at levels comparable with WT barttin-mCFP were localized within or in close proximity to the plasma membrane (Fig. 1*D*). Fig. 1*E* summarizes the results on barttin stability and expression in a topology model.

CLC-K subunits exhibit two potential glycosylation sites (5) and can exist in non-, core-, or complex-glycosylated forms (14, 15). CLC-K is mainly non- or core-glycosylated in the absence of barttin. The accessory subunit barttin promotes CLC-K complex-glycosylation which stimulates surface membrane insertion of CLC-K and protects against protein degradation (14, 15). Complex-glycosylation of the channel thus permits a simple quantitative parameter to test whether mutant barttin functionally interacts with the pore-forming subunit. We co-transfected MDCKII cells with plasmids encoding YFP-hClC-Ka and WT or mutant barttin-mCFP and studied the effect of barttin on the glycosylation of hClC-Ka (Fig. 2*A*). Fig. 2*B* provides a quantitative analysis of hClC-Ka glycosylation when co-expressed with tryptophan-substituted barttin. With the exception of L18W, every barttin mutant that expresses at levels comparable to WT caused a significant increase of hClC-Ka complex-glycosylation as compared with cells expressing the pore-forming subunit alone (Fig. 2, *A* and *B*). These results demonstrate that insertions of individual tryptophans do not abolish association of barttin to CLC-K.

Whereas hClC-Ka resides mostly in the endoplasmic reticulum when expressed alone, co-expression with WT barttin causes predominant localization of the channel in or close to the plasma membrane (14). Confocal images of MDCKII cells expressing hClC-Ka without or with mutant barttin provide qualitative insights into modification of CLC-K channel trafficking by barttin and into interaction between barttin and hClC-Ka. For the majority of tryptophan-substituted barttins, we observed a hClC-Ka distribution similar to cells expressing WT barttin. Fig. 2*C* provides examples of cells co-expressing hClC-Ka with WT or mutant barttin.

To quantify the fraction of channels inserted into the plasma membrane, we labeled surface membrane integrated proteins with biotin from the extracellular side and separated them from proteins of intracellular compartments by precipitation with NeutrAvidin-coated beads (15, 26). The number of channel subunits in the surface membrane was determined by measuring the fluorescence intensity of eluted biotin-labeled barttin-mCFP or YFP-hClC-Ka fusion proteins after SDS-PAGE gel analysis (Fig. 2*D*). In all experiments the integrity of cells was tested by biotinylation of the endogenous intracellular protein GAPDH. We only analyzed results from experiments in which no biotin-labeled GADPH could be identified by Western blot analysis. In the absence of barttin, CLC-K channels were inserted in the surface membrane mainly in their non- (Fig. 2*D*, ○) or core-glycosylated form (Fig. 2*D*, ●) (15). Co-expression of WT and mutant barttin increased the fraction of complex-glycosylated protein (Fig. 2*D*, #), but there were also non- and core-glycosylated channels present in the plasma membrane. These experiments confirm earlier studies which demonstrated that CLC-K proteins can be inserted into the surface membrane without complex-glycosylation (15), possibly bypassing the Golgi apparatus (28). Similar results have been reported also for other membrane proteins (29–31).

We determined the fraction of channel subunits in the surface membrane by dividing fluorescence intensities of eluted fusion proteins (Fig. 2*D*) by the fluorescence intensity of the corresponding proteins in the cleared lysate. Ratios were nor-

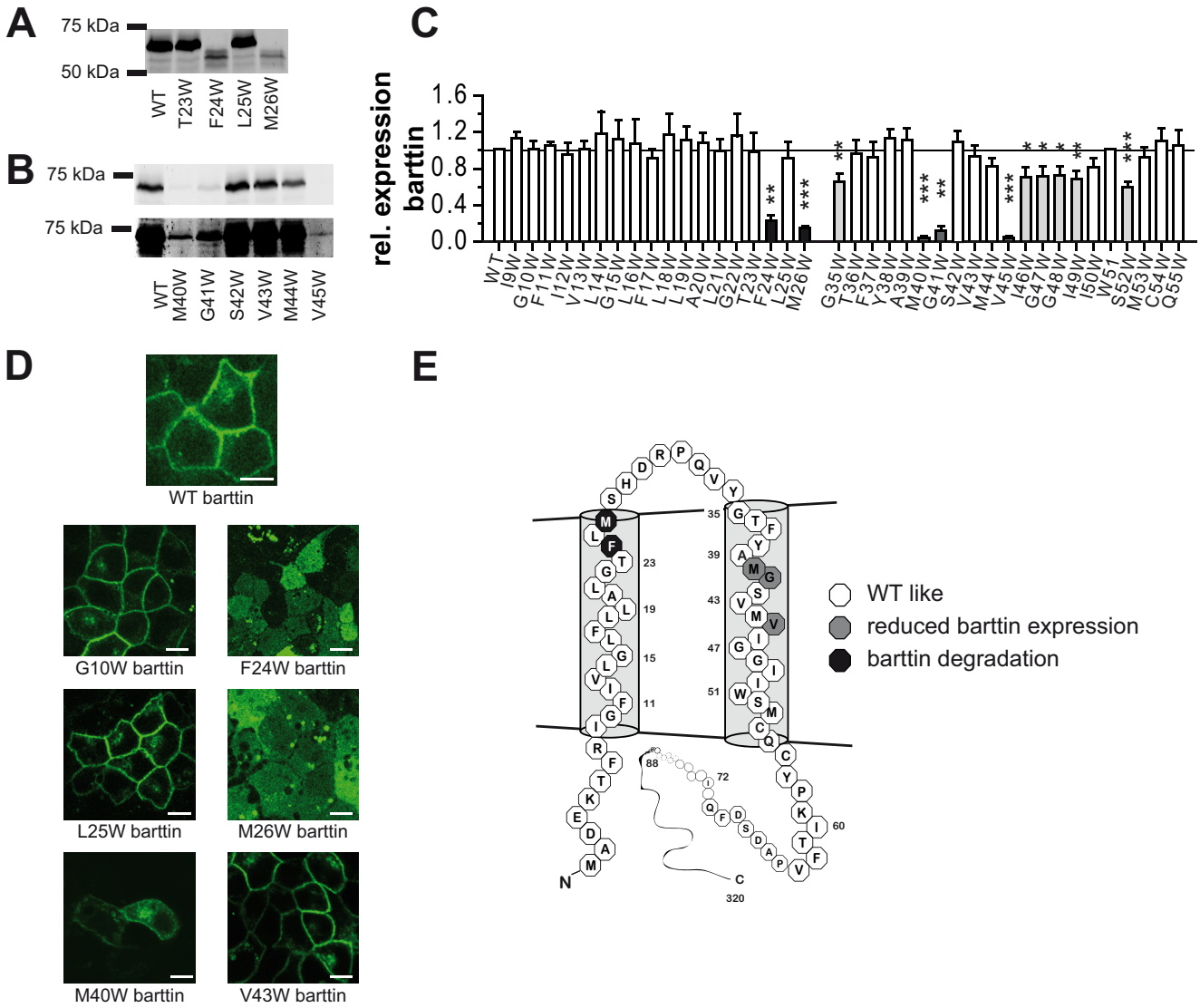

FIGURE 1. **Tryptophan substitutions at most transmembrane residues leave expression and surface membrane insertion of mutant barttin unaffected.** *A* and *B*, fluorescence scan of SDS-PAGE gels of total lysates of HEK293T cells expressing mCFP fusion proteins of WT or selected mutant barttin. In *B* the same gel is scanned at two different intensities (the *lower panel* corresponds to longer exposure time to visualize bands of M40W, G41W, and V45W barttin). *C*, relative expression levels of mutant barttins normalized to WT barttin. Student's *t* test; *, $p < 0.05$; **, $p < 0.01$; ***, $p < 0.001$. $n = 3$–16. All data are mean values ± S.E. *D*, representative confocal images of MDCKII cells expressing WT or mutant barttin-mCFP. *Scale bar* = 10 nm. *E*, topology model of barttin that summarizes the effects of tryptophan substitutions on barttin stability and expression.

malized to values obtained from cells expressing WT barttin in the same series of experiments (Fig. 2*E*). With the exception of misfolded or low expressing mutants, every tryptophan-substituted barttin mutant was inserted into the plasma membrane to a comparable extent as WT barttin (Fig. 2*E*; *upper panel*). However, six mutants failed to effectively promote surface membrane insertion of the hClC-Ka subunit (I12W, G15W, A20W, G48W, S52W, and Q55W) and resulted in significant reduction of the fraction of CLC-K protein accessible to biotinylation (Fig. 2*E*, *lower panel*, *blue bars*). The effects of barttin tryptophan substitution on CLC-K trafficking are summarized in Fig. 2*F* with positions that affect hClC-Ka/barttin trafficking marked in *blue*. Because no unambiguous conclusions about changes in barttin or CLC-K/barttin trafficking can be made for barttin mutations that severely affect barttin stability or expression, these positions are depicted as transparent circles in the barttin topology model.

Effects of Tryptophan Scanning Mutagenesis on hClC-Ka/Barttin Channel Function—Human CLC-K channels are nonconducting in the absence of barttin, and association with the accessory subunit switches these channels into an active state (14, 16). Many tryptophan insertion mutations caused dramatic changes in the function of hClC-Ka/barttin channels (Fig. 3). Fig. 3*A* shows representative whole-cell current recordings from cells expressing hClC-Ka either alone or together with WT, F11W, or F37W barttin. Expression of hClC-Ka alone does not result in any measurable chloride current. When co-transfected with WT barttin, robust anion currents are recorded that instantaneously rise upon voltage steps and deactivate at negative potentials on a very fast time scale (15, 16, 18). This particular gating results in a characteristic hook-shaped current-voltage relationship for hClC-Ka/barttin whole-cell currents (Fig. 3*B*).

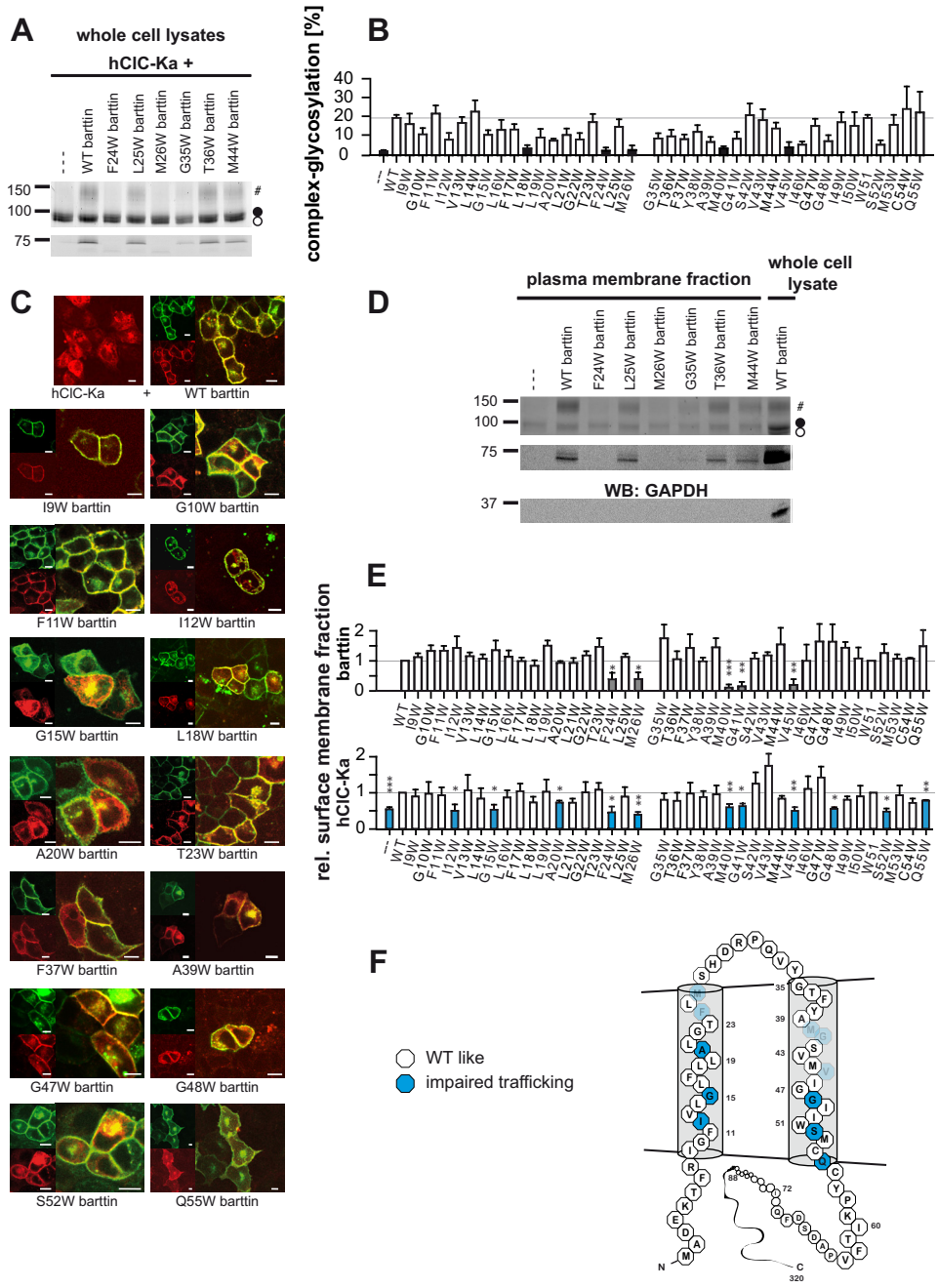

FIGURE 2. **Effects of tryptophan mutations on post-translational modification and trafficking of hClC-Ka/barttin.** *A*, fluorescent SDS-PAGE gels of whole cell lysates from cells expressing hClC-Ka (*upper panel*) together with WT or selected mutant barttin (*lower panel*). For all samples total protein concentrations were adjusted to the same level. In SDS-PAGE gels, three hClC-Ka bands are visible that correspond to non-glycosylated (○), core-glycosylated (●), and complex-glycosylated (#) channel protein. *B*, ratio of complex-glycosylated to total YFP-hClC-Ka fluorescence intensities from cells co-expressing WT or mutant barttin ($n = 3–49$). All data are mean values ± S.E. Student's *t* test *versus* hClC-Ka with/without barttin; *black bars*, $p > 0.05$). *C*, representative confocal images of barttin-mCFP mutants (*green*) co-expressed with YFP-hClC-Ka (*red*) in MDCKII cells. *D*, fluorescent SDS-PAGE gels of the surface membrane exposed fraction (eluates) from cells expressing hClC-Ka (*upper panel*) together with WT or selected mutant barttin (*middle panel*). Non-glycosylated (○) and core-glycosylated (●) as well as complex-glycosylated (#) channel proteins were surface-biotinylated. For all samples total protein concentrations were adjusted to the same level. Western blot analysis of the gel using anti-GAPDH antibodies (*WB*, *lower panel*) validates exclusive biotinylation of surface membrane proteins. *E*, relative surface membrane fraction calculated as the ratios of normalized eluate and lysate band intensities for cells expressing WT and mutant barttin (*upper bar chart*) together with hClC-Ka (*lower bar chart*; $n = 3–29$. All data are the mean values ± S.E. Student's *t* test *versus* values obtained with WT barttin. *, $p < 0.05$; **, $p < 0.01$; ***, $p < 0.001$). *Horizontal lines in B* and *E* provide glycosylation and surface membrane insertion levels obtained with WT barttin. *F*, consequences of tryptophan substitutions on barttin stability and intracellular trafficking of hClC-Ka are summed in a topology model. Misfolded/degraded mutant barttins or barttins that express at low levels are depicted as *transparent circles*.

Fig. 3*C* compares macroscopic hClC-Ka/barttin current amplitudes at +105 mV for WT and mutant barttin. A large number of tryptophan insertions abolished (Fig. 3*C*, *black bars*, G10W, I12W, V13W, L14W, G15W, F17W, L18W, A20W, L21W, G22W, T23W, F24W, L25W, M26W, T36W, G41W, M44W, V45W, G48W, and C54W barttin) or reduced (*yellow bars*, F37W, M40W, G47W, and Q55W barttin) hClC-Ka/barttin currents. To test whether these reduced macroscopic cur-

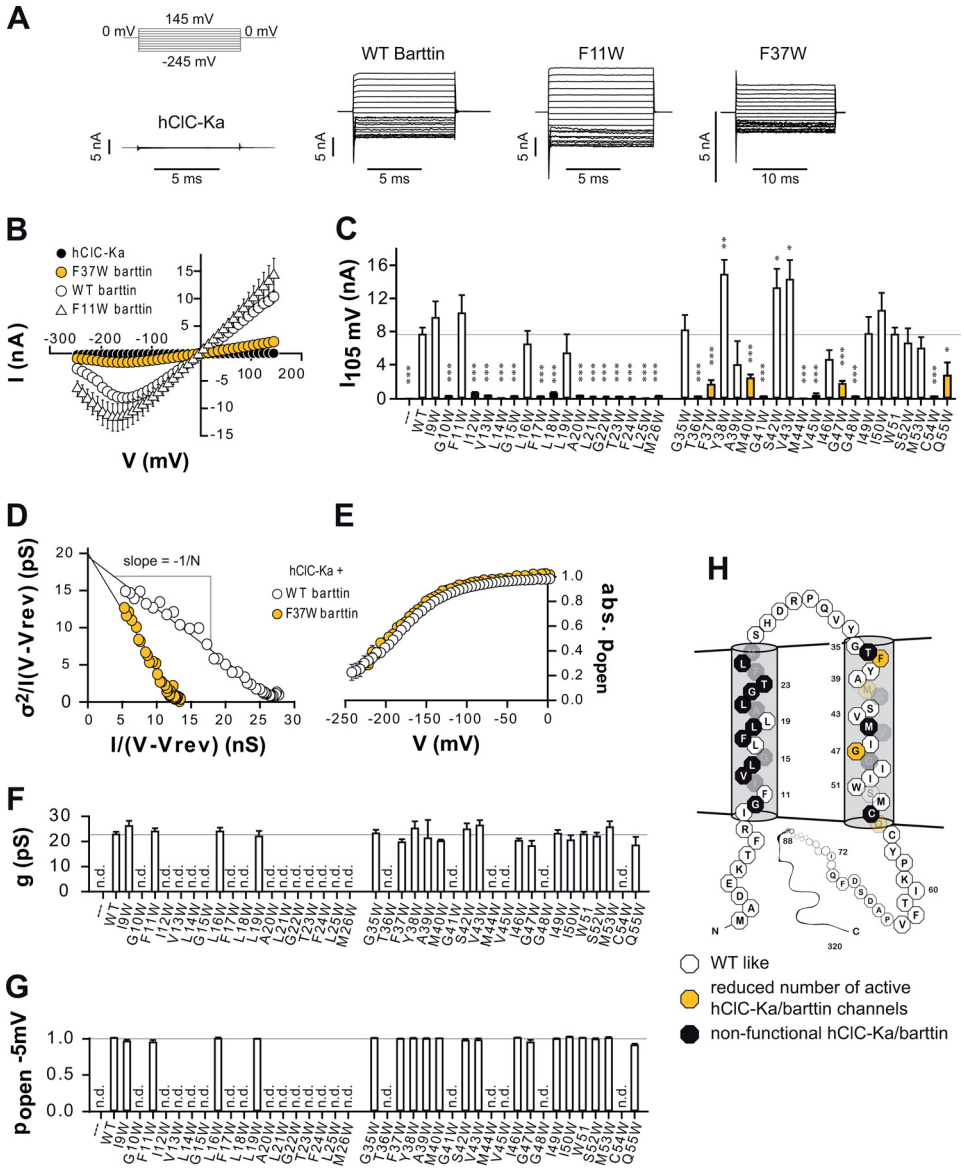

FIGURE 3. **Functional consequences of barttin tryptophan substitution on hClC-Ka/barttin currents.** *A* and *B*, voltage protocol, representative current traces (*A*) and current-voltage relationships (*B*) of whole cell recordings of HEK293T cells expressing hClC-Ka together with WT or representative barttin mutants. *C*, comparison of mean current amplitudes at +105 mV with regular (*white*) and significantly reduced (*yellow*) or absent (*black*) chloride currents. *D*, representative noise analyses for hClC-Ka co-expressed with WT or F37W barttin. Steady-state variances at different voltages were normalized by the product of current amplitude and driving force and plotted *versus* the macroscopic conductance. In this plot, the *y* axis intercept of the linear regression corresponds to the unitary conductance, and the slope corresponds to the number of active channels in the membrane. *E*, voltage dependence of absolute open probabilities for hClC-Ka co-expressed with WT and F37W barttin. *F* and *G*, unitary conductance (*F*; *pS*, picosiemens) and absolute open probability p_{open} at −5 mV (*G*) of hClC-Ka/barttin for WT and mutant barttin (*n.d.* = not determinable). All data in *B*–*G* (except *D*) are the mean values ± S.E. Student's *t* test *versus* WT barttin. $n = 4–32$. *, $p < 0.05$; **, $p < 0.01$; ***, $p < 0.001$). *Horizontal lines* in *C*, *F*, and *G* give mean current amplitude, unitary conductance, or absolute open probability obtained with WT barttin. *H*, the effects of barttin tryptophan insertion on hClC-Ka/barttin mapped onto the topology model of barttin. Misfolded mutant barttins or barttins that express either at low levels or impair ClC-K insertion into the surface membrane are depicted as transparent circles.

rent amplitudes are caused by changes in the function of individual CLC-Ka/barttin channels, we performed stationary noise analysis.

Fig. 3*D* depicts representative noise analyses for hClC-Ka/WT barttin and hClC-Ka/F37W barttin. Stationary current variances at voltages between −245 and 0 mV were normalized by the product of the mean current amplitude (I) and the electrical driving force ($V - V_{rev}$) and plotted *versus* the macroscopic conductance (32). A linear fit to these data provides the unitary current conductance as *y* axis intercept and the number of channels as inverse slope factor (16, 18, 32). From these two parameters, the absolute open probability can be calculated from steady-state current amplitudes at various potentials (Fig. 3*E*). Noise analysis reveals unchanged unitary current amplitudes and absolute open probabilities of hClC-Ka/F37W barttin.

For 4 of 18 mutations within TM1 and 14 of 20 mutations within TM2 hClC-Ka/barttin current amplitudes were large enough for noise analysis. None of these barttin mutations altered unitary channel properties (Fig. 3, *F* and *G*). Mutations that reduced mean current amplitudes (F37W, M40W, G47W, and Q55W barttin) left single channel conduction and open

probability unaffected and reduced the number of active channels. For M40W and Q55W these findings can be explained by the reduced surface insertion probability of hClC-Ka/mutant barttin channels (Fig. 2*E*). However, unchanged numbers of hClC-Ka/barttin in the surface membrane have been determined for F37W and G47W barttin (Fig. 2). This apparent contradiction can be explained by the different detection methods. Whereas biochemical and microscopic methods cannot distinguish between active and inactive channels, noise analysis only detects channels that open or close during the observation time. The unaltered subcellular distribution together with the reduced current amplitudes thus suggest gating processes in hClC-Ka/mutant barttin channels that are too slow to be observed by noise analysis. Such gating processes will cause the closures of a fraction of the channel for long time periods and result in an apparent reduction of active channels determined by noise analysis. One possible mechanism would be that the hClC-Ka slow gate, which is fully opened in hClC-Ka/WT barttin channels (16), dwells in long-lasting closed states in channels associated with mutant barttin. Alternatively, tryptophan insertion at certain positions might impair proper maturation of ClC-Ka channels, so that a percentage of channels is not switched into a conducting conformation.

These scenarios also provide possible explanations for various mutant barttins that abolish hClC-Ka/barttin currents, without affecting their surface membrane insertion (G10W, V13W, L14W, F17W, L18W, L21W, G22W, T23W, L25W, T36W, M44W, and C54W barttin). We conclude that a large number of tryptophan insertion mutants affect the function of hClC-Ka/barttin channels but leave their subcellular distribution unaffected.

In the topology model that summarizes the effects of tryptophan substitutions on distinct channel properties (Fig. 3*H*), we distinguish a tryptophan insertion that reduces the number of active channels (marked in *yellow*) from those that completely abolish channel function (marked in *black*). For barttin mutations that alter barttin expression and/or CLC-K/barttin trafficking (transparent circles), we cannot make clear conclusions about effects on channel function and, therefore, excluded them from this analysis.

Tryptophan Insertions Modify Gating of rClC-K1/Barttin—In contrast to human hClC-Ka and hClC-Kb and rat rClC-K2, which are only functional in the presence of barttin, rClC-K1 channels are conductive also in the absence of barttin (2, 14, 33). Similar to other CLC channels (34–39), CLC-K chloride channels exhibit two ion conduction pathways that are opened and closed either individually by fast gating or jointly by slow cooperative gating processes (16). Barttin modifies voltage-dependent gating of rClC-K1 by constitutively activating the slow common gate of these channels (16). Barttin-induced changes in rClC-K1 gating are particularly prominent and easy to quantify for V166E rClC-K1. In this mutation a neutral valine within a conserved motif ($GK^E/_VGP$) at the amino terminus of the F helix (40) was substituted by glutamate.

We used experiments on V166E rClC-K1 to quantify the effects of tryptophan insertion mutagenesis on gating modification by barttin. For V166E rClC-K1, fast and slow gating can be separated by voltage step protocols in which a 5-ms voltage step to +180 mV is inserted between a variable prepulse and a test step to a fixed potential of −125 mV (16). The short depolarization fully opens the fast gate without significant alteration of slow common gating so that the isochronal tail current amplitudes depend only on the relative open probability of the slow gate. Dividing the total open probability of the channel by the slow gate open probability provides the activation curve of the fast gate (Fig. 4*A*). Barttin modifies the time course of V166E rClC-K1 currents by constitutively opening the slow gate and shifting the fast gate activation curve to more negative potentials (Fig. 4*B*) (16).

Fig. 4, *C–F*, shows representative current recordings from cells co-expressing V166E rClC-K1 with tryptophan-substituted barttins. Whereas V43W barttin exerts similar effects on V166E rClC-K1 gating as WT barttin (Fig. 4*C*), gating of V166E rClC-K1/T36W barttin (Fig. 4*D*) resembles the behavior of channels expressed without barttin. Cells co-expressing V166E rClC-K1 with A39W barttin (Fig. 4*E*) display anion currents that resemble a superposition of channels with and without barttin. I12W and G15W cause a dramatic reduction of V166E rClC-K1/barttin current amplitudes (Fig. 4*F*).

To quantify the effects of barttin tryptophan insertion, we compared macroscopic current amplitudes of cells expressing V166E rClC-K1/barttin at +125 mV and −155 mV (Fig. 4*G*), the midpoint of fast activation (Fig. 4*H*), and the voltage-dependent component of slow gating for all barttin substitutions (Fig. 4*I*). Tryptophan insertions modified V166E rClC-K1/barttin macroscopic current amplitudes (Fig. 4*G*) at similar, but not identical residues, as hClC-Ka/barttin (Fig. 3*C*). Separation of fast and slow gate activation demonstrated distinct effects of barttin mutations on fast and on slow gating. Besides L14W, all mutations within TM1 either left fast gating unaffected or resulted in voltage-independent fast gating that prevented determination of the midpoint of activation (Fig. 4*H*). Within TM1 and TM2, tryptophan insertion at the majority of residues resulted in voltage-dependent changes in slow gating of V166E rClC-K1/barttin, indicating that these mutations impaired constitutive activation of the slow gate as a function of WT barttin (Fig. 4*I*). These changes in fast and/or slow gating do not predict the observed changes in absolute current amplitudes (Fig. 4*G*). For some mutations, current amplitudes were dramatically reduced, suggesting much lower absolute open probabilities of V166E rClC-K1 associated with tryptophan-inserted barttin than for barttin-free channels.

We used the three functional parameters (Fig, 4, *G–I*) to sort the tryptophan substitution mutations into different groups. The first group consists of tryptophan insertion mutations that left V166E rClC-K1/barttin in all gating aspects unaffected (L16W, L19W, G35W, F37W, Y38W, V43W, I46W, I50W, and M53W). These mutations are marked as *white circles* in the topology model in Fig. 4*J*. Mutations that led to missing regulation of V166E rClC-K1 gating (*red*; T36W and M44W barttin) represent a second group. The lack of gating modification by these two barttin

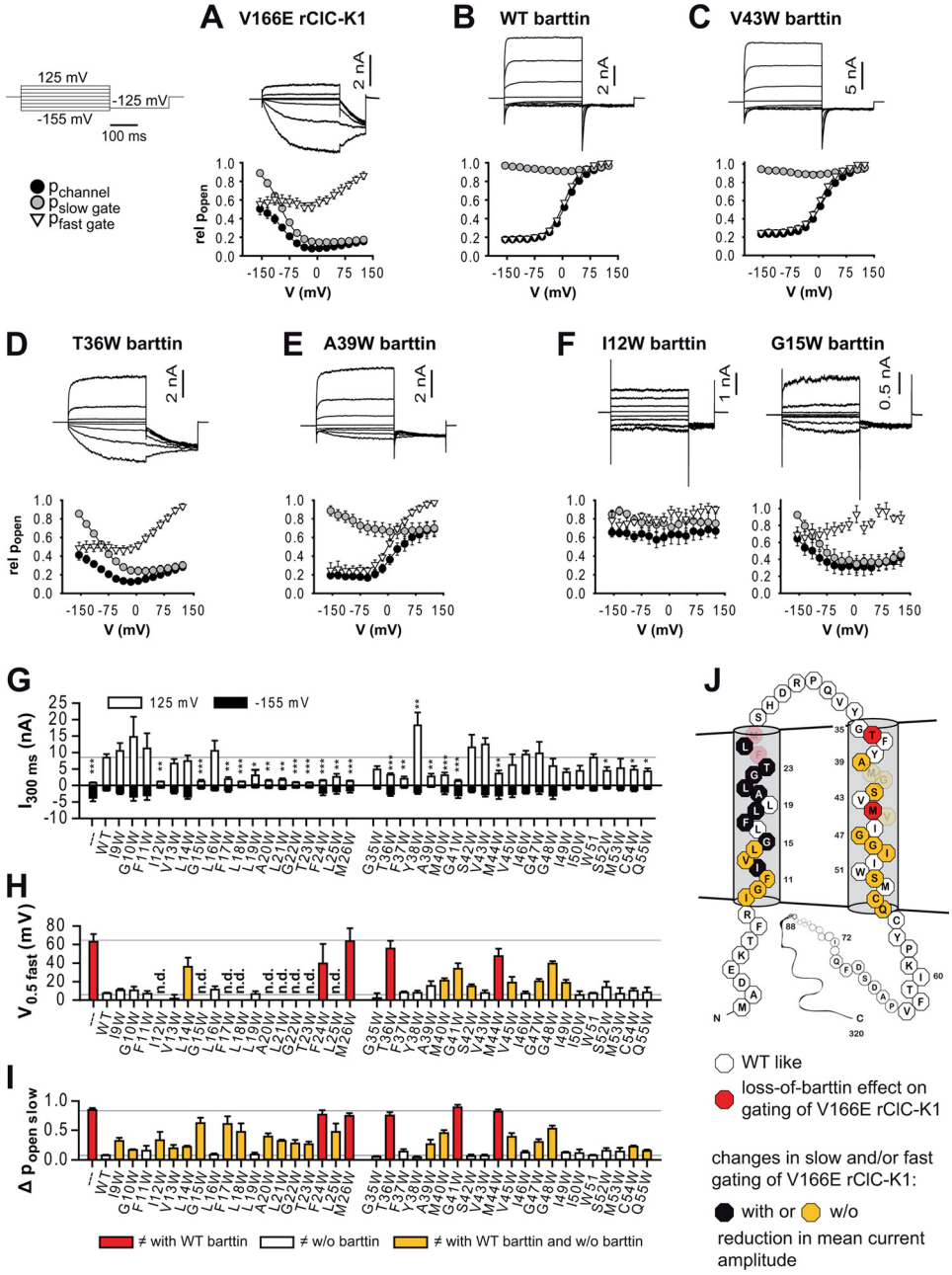

FIGURE 4. **Tryptophan substitutions alter the voltage dependence of V166E rClC-K1/barttin.** *A–F*, whole cell current recordings and activation curves from HEK293T cells expressing V166E rClC-K1 without (*A*) or with WT (*B*) or selected mutant (*C–F*) barttin. *G–I*, comparison of steady-state mean current amplitudes. Data are the mean values ± S.E. $n = 4–15$. Student's *t* test for values at +125 mV *versus* WT barttin. *, $p < 0.05$; **, $p < 0.01$; ***, $p < 0.001$) (*G*), midpoint of fast gate activation $V_{0.5\ fast}$ (*H*), and $\Delta p_{slow\ gate}$ (*I*) of V166E rClC-K1 co-expressed with WT or mutant barttin. *H–I*, data are the mean values ± S.E. $n = 4–15$. Two separate Student's *t* tests reveal significant differences to values obtained in the absence or presence of WT barttin as indicated by the color-coded bars. $p < 0.05$). *Horizontal lines* (*G–I*) provide levels obtained with or without WT barttin. *J*, topology model of barttin summarize the results of barttin tryptophan substitution on V166E rClC-K1 gating. Misfolded/degraded mutant barttins or barttins that express at low levels are depicted as *transparent circles*.

mutants is probably not due to abolished interaction with CLC-K channels as demonstrated by increased complex-glycosylation (Fig. 2*B*) and surface membrane insertion (Fig. 2*E*) of hClC-Ka. Barttin mutants that alter gating of V166E rClC-K1/barttin either by affecting the voltage dependence of fast (Fig. 4*H*) or slow gating (Fig. 4*I*) were classified in a third group (marked in *yellow*). A last group encompasses barttin mutants that result in very low macroscopic current amplitudes upon depolarization and hyperpolarization (<1.7 nA at +125 mV and <−1 nA at −155 mV; marked as *black circles* in Fig. 4*J*).

Discussion

Barttin is an accessory subunit that is necessary for normal function and subcellular localization of CLC-K channels. The high physiological importance of CLC-K channel regulation by barttin is illustrated by naturally occurring barttin mutations found in patients with sensorineural deafness, in most cases

combined with impaired urinary concentration, hyponatremia, hypovolemia, and hypotension (10, 15, 18, 41–43). At present, the CLC-K-barttin interaction is sufficiently understood at neither the mechanistic nor the structural level. Multiple functions of barttin have been described, but it is still unclear how an accessory subunit can modify intracellular trafficking and protein stability as well as ion channel gating and conduction.

We employed serial perturbation mutagenesis to identify the sequence requirements for the distinct barttin functions. We inserted individual tryptophan residues at each position of predicted transmembrane domains (10, 11) and studied the effects of these mutations on barttin biogenesis and trafficking as well as on CLC-K glycosylation, trafficking, and function. Without barttin, a large percentage of CLC-K is retained in the endoplasmic reticulum, and barttin promotes surface channel membrane insertion (13, 14). We tested the effects of tryptophan insertion on barttin-mediated endoplasmic reticulum exit of CLC-K channels by studying the glycosylation pattern, confocal imaging, and surface biotinylation (Fig. 2) (14, 15). In the absence of barttin, hClC-Ka is non-conducting, and barttin is required to convert it into a functional anion channel (14). V166E rClC-K1 is active also without barttin (2, 14), but barttin modifies its voltage-dependent gating (14, 16). In the present study the functional modification of CLC-K channels by mutant barttin was studied by quantifying macroscopic chloride current amplitudes as well as voltage-dependent gating of CLC-K/barttin channels using whole-cell patch clamp recordings in transfected cells (Figs. 3 and 4).

Barttin tolerates substitutions of most transmembrane amino acids by tryptophan. The majority of mutant barttins could be resolved as full-length protein in SDS-PAGE gels and inserted into the plasma membrane as shown by confocal imaging and biotinylation (Figs. 1 and 2). For F24W and M26W barttin, the translated protein is misfolded and/or proteolytically degraded, and co-expression of these mutant proteins did not modify trafficking or function of hClC-Ka and V166E rClC-K1. Expression levels of M40W, G41W, and V45W barttin are dramatically reduced. The five residues might be important for protein biogenesis and/or stability, possibly by mediating the interaction between TM1 and TM2.

For all tryptophan-substituted barttins that were correctly folded, we could demonstrate functional interaction with CLC-K channels either by increasing the percentage of complex-glycosylated protein, by changes in the percentage of surface-biotinylated CLC-K, or by modification of functional properties of hClC-Ka and/or V166E rClC-K1. Even the three mutant barttins that express only at very low levels, M40W, G41W, and V45W barttin, modify channel function of hClC-Ka (Fig. 3, *F* and *G*) and/or V166E rClC-K1 (Fig. 4, *G–I*), demonstrating that these mutants interact with pore-forming CLC-K subunits. Taken together, these results suggest that none of the mutations abolishes association of barttin to CLC-K, most likely because barttin binds to CLC-K via interaction of multiple side chains.

We observed pronounced differences in the effects of individual tryptophan insertions on CLC-K/barttin trafficking and function. The majority of the tryptophan insertions left trafficking of CLC-K/barttin unaffected (Fig. 2), indicating that association of barttin to CLC-K is sufficient for normal trafficking. In contrast, many mutations affected hClC-Ka/barttin and V166E rClC-K1/barttin functions, suggesting that specific interactions of barttin with CLC-K, which can be impaired by single point mutations, are required for functional channel modification. Within TM1, nine tryptophan insertions abolish hClC-Ka/barttin currents by preventing channel activation. Within TM2, two mutant barttins, F37W and G47W barttin, result in reduced mean current amplitude of hClC-Ka/barttin, and three mutations, T36W, M44W, and C54W, abolish hClC-Ka activation despite normal trafficking of barttin or hClC-Ka/barttin. Barttin modifies specific gating properties of V166E rClC-K1 (12, 14, 16), and we used this isoform to get further mechanistic insights into the functional modification of CLC-K. We initially quantified the functional modification of V166E rClC-K1 by barttin by separating fast and slow gating. Besides mutations that either left gating modification of V166E rClC-K1 unaffected or completely abolished this barttin function, we found several tryptophan insertion mutations that resulted in specific alterations of the voltage dependence of fast or/and slow gating. Moreover, there are barttin mutants that dramatically reduce the whole-cell current amplitude even below amplitudes recorded without barttin. This current reduction is most likely due to a diminished absolute open probability. All these inactivating mutant barttins resulted from amino acid exchanges within TM1, thus further supporting the notion that tryptophan insertions within TM1 result in more severe changes of function than substitutions within TM2.

Fig. 5 shows helical wheel representations of the different effects of tryptophan substitutions in barttin, *i.e.* function of hClC-Ka/barttin and V166E rClC-K1/barttin (Fig. 5*A*) or barttin expression and intracellular CLC-K/barttin trafficking (Fig. 5*B*). Because the effects of tryptophan insertion on trafficking cannot always be unambiguously separated from the effects in function, we did not consider barttin mutants with much lower expression levels or reduced CLC-K/barttin insertion in Fig. 5*A*. Within TM1 the majority of tryptophan insertions abolishes hClC-Ka/barttin function and modifies V166E rClC-K1/barttin gating (Fig. 5*A*). Assuming a helical arrangement of TM1, a cluster of hydrophobic residues can be identified that appears to be necessary for hClC-Ka activation. Barttin function appears to be less sensitive to tryptophan insertion mutagenesis within TM2 with only three tryptophan insertions that abolish function of hClC-Ka (T36W, M44W, and C54W). For V166E rClC-K1/barttin, several tryptophan insertions within TM2 caused only mild changes in the voltage dependence of fast and/or slow gating (A39W, S42W, G47W, I49W, and C54W). The prominent effects of tryptophan insertions within TM1 and the fact that many of these residues project side chains in the same direction suggest that these amino acids contribute to the binding interface with CLC-K. Tajima *et al.* (44) demonstrated binding of barttin to isolated B and J helices of CLC-K. The presence of multiple leucines and other hydrophobic domains within these channel helices together with the dominance of hydrophobic amino acid side chains within TM1

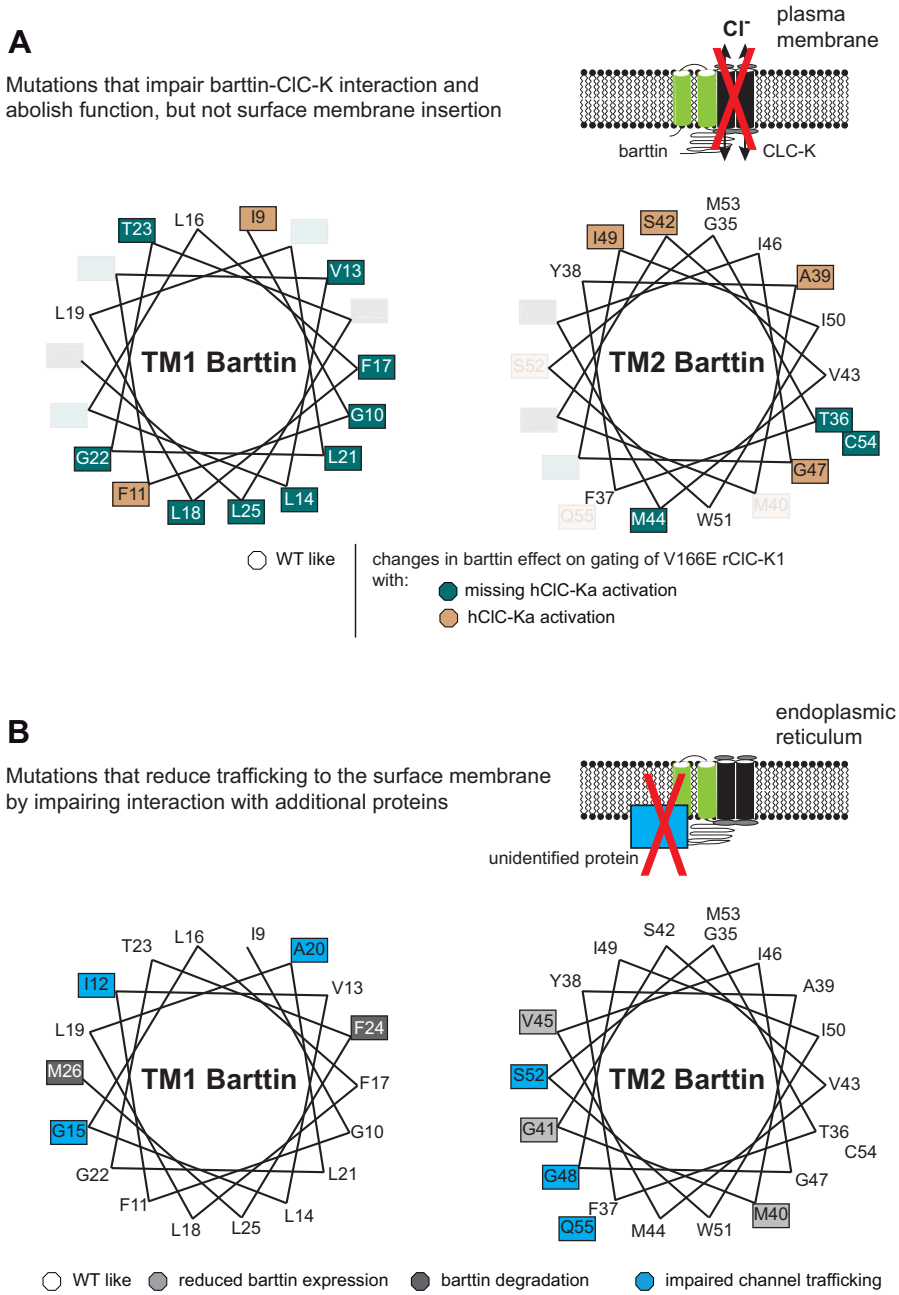

FIGURE 5. **Helical wheel projection identifies a potential interface for interaction with CLC-K pore-forming subunits.** *A* and *B*, schematic illustration of the two-tiered mechanisms of CLC regulation by barttin and helical wheel models for barttin assuming an α-helical (3.6 amino acids per turn) organization of TM1 and TM2. Residues are color-coded corresponding to the results on hClC-Ka activation and gating regulation of V166E rClC-K1 in *A* and barttin expression and chaperone function in *B*. Chaperone-deficient and low expressing or degraded barttin mutants are transparent in *A*.

of barttin suggest that barttin binds via leucine zipper motifs to CLC-K. Tryptophan insertion into this binding domain likely modifies the interaction of barttin with the pore-forming CLC-K subunit and alters channel function. One might speculate that mutations within TM2 modify the interaction of TM1 with CLC-K. Alternatively, TM2 might also bind to CLC-K or even to other so-far not identified proteins that might be part of the CLC-K/barttin complex. The subunit stoichiometry of the CLC-K/barttin complex has not yet been determined. It is, therefore, also possible that some of the contacts affected by tryptophan insertion are between two different barttin molecules.

Our results provide first mechanistic insights into the different effects of barttin on CLC-K trafficking and function. None of the mutations in Fig. 5*A* impaired the association of barttin to CLC-K in a way to prevent complex-glycosylation, endoplasmic reticulum exit, and surface membrane insertion. However, there are several mutations that weaken the interaction sufficiently to prevent functional modification of CLC-K. These findings support a two-tiered regulation mechanism of CLC-K by barttin. Tight interaction appears necessary to cause the specific functional barttin effects on CLC-K channels (16). However, even weakened interaction suffices for barttin's effects on channel glycosylation and trafficking.

There are other residues at which tryptophan insertion impairs intracellular trafficking, with less pronounced effects on function. Mutant barttins that affect intracellular transport of hClC-Ka (Fig. 5*B*, *blue*) are often close to the cytoplasmic parts of barttin (I12W, G15W, S52W, and Q55W) and possibly modify the interaction with targeting signals from cytoplasmic proteins or cytoplasmic domains of membrane-inserted binding partners. Moreover, three TM2 positions at which tryptophan insertions affect channel trafficking project into the same direction, indicating a potential binding pocket for other membrane proteins involved in intracellular channel transport and targeting.

Barttin exerts different effects on hClC-Ka and rClC-K1 function. Analysis of naturally occurring *BSND* mutations (15) demonstrated that several mutant barttins failed to activate hClC-Ka but were still capable of modifying V166E rClC-K1 gating. This finding suggested that these two functional effects of barttin might be mediated by distinct protein regions. We here exploited serial perturbation mutagenesis and the distinct regulation of rClC-K1 by barttin to address this question. Because V166E rClC-K1 does not require barttin to be functional, we can separate the effects of barttin on CLC-K/barttin maturation, intracellular transport, and CLC-K function. We found every mutant that impairs hClC-Ka function also affects gating and/or absolute open probability of V166E rClC-K1. These results support the notion that barttin switches hClC-K channels from a non-conducting into an active form by modifying gating. Because hClC-Ka/barttin channels exhibit voltage-dependent protopore gating (16) and an open cooperative slow gate and because barttin constitutively opens the slow gate of rClC-K1, we conclude that hClC-Ka channels are closed by the slow gate in the absence of barttin.

Dramatic differences in channel gating (16, 45) and pharmacology (25) have been reported between CLC-K/barttin channels expressed in *Xenopus* oocytes or in mammalian cells. Whereas hClC-Ka/barttin exhibits open probabilities close to 1 in mammalian cells (18), comparable measurements in *Xenopus* oocytes reveal values too small to be accurately measured (45). Moreover, whereas niflumic acid potentiates hClC-Ka/barttin currents in oocytes, such an effect is absent in mammalian cells (25). These differences in channel properties in separate expression systems suggest that additional factors, such as yet unidentified subunits or modifying factors (37), might alter gating of CLC-K/barttin channels. If there were additional subunits of the CLC-K/barttin complex, it appears possible that some of the side chains identified in tryptophan scanning mutagenesis might interact with these proteins. It will be interesting to see the effects of the tryptophan scanning in the *Xenopus* expression systems. The results of such experiments together with those of the present study will provide novel insights into the molecular basis of the functional differences of CLC-K/barttin channels expressed in mammalian cells or amphibian oocytes.

In summary, tryptophan scanning mutagenesis combined with electrophysiological, biochemical, and microscopic analysis permitted identification of residues that are essential for distinct barttin functions. Our work identified a binding motif within TM1 for a potential binding partner in the CLC-K B helix. Moreover, we could demonstrate a two-step modification of CLC-K channels by barttin, with association conferring endoplasmic reticulum exit and surface membrane insertion and tight interactions of TM1 with yet to be defined regions within CLC-K for functional modification.

Acknowledgments—We thank Drs. Shinichi Uchida and Al George for providing the expression constructs for rClC-K1, hClC-Ka, and barttin, Drs. Patricia Hidalgo, Stefanie Bungert-Plümke, and Gabriel Stölting for helpful discussions, and Toni Becher, Birgit Begemann, and Petra Kilian for excellent technical assistance.

References

1. Stölting, G., Fischer, M., and Fahlke, Ch. (2014) CLC channel function and dysfunction in health and disease. *Front Physiol* **5,** 378
2. Uchida, S., Sasaki, S., Furukawa, T., Hiraoka, M., Imai, T., Hirata, Y., and Marumo, F. (1993) Molecular cloning of a chloride channel that is regulated by dehydration and expressed predominantly in kidney medulla. *J. Biol. Chem.* **268,** 3821–3824
3. Adachi, S., Uchida, S., Ito, H., Hata, M., Hiroe, M., Marumo, F., and Sasaki, S. (1994) Two isoforms of a chloride channel predominantly expressed in thick ascending limb of Henle's loop and collecting ducts of rat kidney. *J. Biol. Chem.* **269,** 17677–17683
4. L'Hoste, S., Diakov, A., Andrini, O., Genete, M., Pinelli, L., Grand, T., Keck, M., Paulais, M., Beck, L., Korbmacher, C., Teulon, J., and Lourdel, S. (2013) Characterization of the mouse ClC-K1/Barttin chloride channel. *Biochim. Biophys. Acta* **1828,** 2399–2409
5. Kieferle, S., Fong, P., Bens, M., Vandewalle, A., and Jentsch, T. J. (1994) Two highly homologous members of the ClC chloride channel family in both rat and human kidney. *Proc. Natl. Acad. Sci. U.S.A.* **91,** 6943–6947
6. Uchida, S., Sasaki, S., Nitta, K., Uchida, K., Horita, S., Nihei, H., and Marumo, F. (1995) Localization and functional characterization of rat kidney-specific chloride channel, ClC-K1. *J. Clin. Invest.* **95,** 104–113
7. Matsumura, Y., Uchida, S., Kondo, Y., Miyazaki, H., Ko, S. B., Hayama, A., Morimoto, Liu, W., Arisawa, M., Sasaki, S., and Marumo, F. (1999) Overt nephrogenic diabetes insipidus in mice lacking the CLC-K1 chloride channel. *Nat. Gen.* **21,** 95–98
8. Kobayashi, K., Uchida, S., Mizutani, S., Sasaki, S., and Marumo, F. (2001) Intrarenal and cellular localization of CLC-K2 protein in the mouse kidney. *J. Am. Soc. Nephrol.* **12,** 1327–1334
9. Rickheit, G., Maier, H., Strenzke, N., Andreescu, C. E., De Zeeuw, C. I., Muenscher, A., Zdebik, A. A., and Jentsch, T. J. (2008) Endocochlear potential depends on Cl^- channels: mechanism underlying deafness in Bartter syndrome IV. *EMBO J.* **27,** 2907–2917
10. Birkenhäger, R., Otto, E., Schürmann, M. J., Vollmer, M., Ruf, E. M., Maier-Lutz, I., Beekmann, F., Fekete, A., Omran, H., Feldmann, D., Milford, D. V., Jeck, N., Konrad, M., Landau, D., Knoers, N. V., Antignac, C., Sudbrak, R., Kispert, A., and Hildebrandt, F. (2001) Mutation of BSND causes Bartter syndrome with sensorineural deafness and kidney failure. *Nat. Genet.* **29,** 310–314
11. Estévez, R., Boettger, T., Stein, V., Birkenhäger, R., Otto, E., Hildebrandt, F., and Jentsch, T. J. (2001) Barttin is a Cl^- channel β-subunit crucial for renal Cl^- reabsorption and inner ear K^+ secretion. *Nature* **414,** 558–561
12. Waldegger, S., Jeck, N., Barth, P., Peters, M., Vitzthum, H., Wolf, K., Kurtz, A., Konrad, M., and Seyberth, H. W. (2002) Barttin increases surface expression and changes current properties of ClC-K channels. *Pflugers Arch.* **444,** 411–418
13. Hayama, A., Rai, T., Sasaki, S., and Uchida, S. (2003) Molecular mechanisms of Bartter syndrome caused by mutations in the BSND gene. *Histochem. Cell Biol.* **119,** 485–493
14. Scholl, U., Hebeisen, S., Janssen, A. G., Müller-Newen, G., Alekov, A., and Fahlke, Ch. (2006) Barttin modulates trafficking and function of ClC-K channels. *Proc. Natl. Acad. Sci. U.S.A.* **103,** 11411–11416
15. Janssen, A. G., Scholl, U., Domeyer, C., Nothmann, D., Leinenweber, A., and Fahlke, Ch. (2009) Disease-causing dysfunctions of barttin in Bartter

syndrome type IV. *J. Am. Soc. Nephrol.* **20,** 145–153
16. Fischer, M., Janssen, A. G., and Fahlke, Ch. (2010) Barttin activates ClC-K channel function by modulating gating. *J. Am. Soc. Nephrol.* **21,** 1281–1289
17. Fahlke, Ch., and Fischer, M. (2010) Physiology and pathophysiology of ClC-K/barttin channels. *Front. Physiol.* **1,** 155
18. Riazuddin, S., Anwar, S., Fischer, M., Ahmed, Z. M., Khan, S. Y., Janssen, A. G., Zafar, A. U., Scholl, U., Husnain, T., Belyantseva, I. A., Friedman, P. L., Riazuddin, S., Friedman, T. B., and Fahlke, Ch. (2009) Molecular basis of DFNB73: mutations of *BSND* can cause nonsyndromic deafness or Bartter syndrome. *Am. J. Hum. Genet.* **85,** 273–280
19. Choe, S., Stevens, C. F., and Sullivan, J. M. (1995) Three distinct structural environments of a transmembrane domain in the inwardly rectifying potassium channel ROMK1 defined by perturbation. *Proc. Natl. Acad. Sci. U.S.A.* **92,** 12046–12049
20. Collins, A., Chuang, H., Jan, Y. N., and Jan, L. Y. (1997) Scanning mutagenesis of the putative transmembrane segments of Kir2.1, an inward rectifier potassium channel. *Proc. Natl. Acad. Sci. U.S.A.* **94,** 5456–5460
21. Li-Smerin, Y., Hackos, D. H., and Swartz, K. J. (2000) A localized interaction surface for voltage-sensing domains on the pore domain of a K^+ channel. *Neuron* **25,** 411–423
22. Somasekharan, S., Tanis, J., and Forbush, B. (2012) Loop diuretic and ion-binding residues revealed by scanning mutagenesis of transmembrane helix 3 (TM3) of Na-K-Cl cotransporter (NKCC1). *J. Biol. Chem.* **287,** 17308–17317
23. Chen, H., and Goldstein, S. A. (2007) Serial perturbation of minK in IKs implies an α-helical transmembrane span traversing the channel corpus. *Biophys. J.* **93,** 2332–2340
24. De Feo, C. J., Mootien, S., and Unger, V. M. (2010) Tryptophan scanning analysis of the membrane domain of CTR-copper transporters. *J. Membr. Biol.* **234,** 113–123
25. Imbrici, P., Liantonio, A., Gradogna, A., Pusch, M., and Camerino, D. C. (2014) Targeting kidney CLC-K channels: Pharmacological profile in a human cell line versus *Xenopus* oocytes. *Biochim. Biophys. Acta* **1838,** 2484–2491
26. Nothmann, D., Leinenweber, A., Torres-Salazar, D., Kovermann, P., Hotzy, J., Gameiro, A., Grewer, C., and Fahlke, Ch. (2011) Hetero-oligomerization of neuronal glutamate transporters. *J. Biol. Chem.* **286,** 3935–3943
27. Torres-Salazar, D., and Fahlke, Ch. (2007) Neuronal glutamate transporters vary in substrate transport rate but not in unitary anion channel conductance. *J. Biol. Chem.* **282,** 34719–34726
28. Grieve, A. G., and Rabouille, C. (2011) Golgi bypass: skirting around the heart of classical secretion. *Cold Spring Harb. Perspect. Med.* 10.1101/cshperspect.a005298
29. Tauber, R., Schenck, I., Josić, D., Gross, V., Heinrich, P. C., Gerok, W., and Reutter, W. (1986) Different oligosaccharide processing of the membrane-integrated and the secretory form of gp 80 in rat liver. *EMBO J.* **5,** 2109–2114
30. Hanwell, D., Ishikawa, T., Saleki, R., and Rotin, D. (2002) Trafficking and cell surface stability of the epithelial Na^+ channel expressed in epithelial Madin-Darby canine kidney cells. *J. Biol. Chem.* **277,** 9772–9779
31. Woo, S. K., Kwon, M. S., Ivanov, A., Geng, Z., Gerzanich, V., and Simard, J. M. (2013) Complex *N*-glycosylation stabilizes surface expression of transient receptor potential melastatin 4b protein. *J. Biol. Chem.* **288,** 36409–36417
32. Sesti, F., and Goldstein, S. A. (1998) Single-channel characteristics of wild-type IKs channels and channels formed with two minK mutants that cause long QT syndrome. *J. Gen. Physiol.* **112,** 651–663
33. Waldegger, S., and Jentsch, T. J. (2000) Functional and structural analysis of ClC-K chloride channels involved in renal disease. *J. Biol. Chem.* **275,** 24527–24533
34. Miller, C. (1982) Open-state substructure of single chloride channels from *Torpedo* electroplax. *Philos. Trans. R. Soc. Lond. B Biol. Sci.* **299,** 401–411
35. Saviane, C., Conti, F., and Pusch, M. (1999) The muscle chloride channel ClC-1 has a double-barreled appearance that is differentially affected in dominant and recessive myotonia. *J. Gen. Physiol* **113,** 457–468
36. Stölting, G., Fischer, M., and Fahlke, Ch. (2014) ClC-1 and ClC-2 form hetero-dimeric channels with novel protopore functions. *Pflügers Archiv.* **466,** 2191–2204
37. Stölting, G., Teodorescu, G., Begemann, B., Schubert, J., Nabbout, R., Toliat, M. R., Sander, T., Nürnberg, P., Lerche, H., and Fahlke, Ch. (2013) Regulation of ClC-2 gating by intracellular ATP. *Pflügers Arch.* **465,** 1423–1437
38. Accardi, A., and Pusch, M. (2000) Fast and slow gating relaxations in the muscle chloride channel CLC-1. *J. Gen. Physiol.* **116,** 433–444
39. Zúñiga, L., Niemeyer, M. I., Varela, D., Catalán, M., Cid, L. P., and Sepúlveda, F. V. (2004) The voltage-dependent ClC-2 chloride channel has a dual gating mechanism. *J. Physiol.* **555,** 671–682
40. Fahlke, Ch., Yu, H. T., Beck, C. L., Rhodes, T. H., and George, A. L., Jr. (1997) Pore-forming segments in voltage-gated chloride channels. *Nature* **390,** 529–532
41. Shalev, H., Ohali, M., Kachko, L., and Landau, D. (2003) The neonatal variant of Bartter syndrome and deafness: preservation of renal function. *Pediatrics* **112,** 628–633
42. Ozlu, F., Yapicioğlu, H., Satar, M., Narli, N., Ozcan, K., Buyukcelik, M., Konrad, M., and Demirhan, O. (2006) Barttin mutations in antenatal Bartter syndrome with sensorineural deafness. *Pediatr. Nephrol.* **21,** 1056–1057
43. Landau, D., Shalev, H., Ohaly, M., and Carmi, R. (1995) Infantile variant of Bartter syndrome and sensorineural deafness: a new autosomal recessive disorder. *Am. J. Med. Genet.* **59,** 454–459
44. Tajima, M., Hayama, A., Rai, T., Sasaki, S., and Uchida, S. (2007) Barttin binds to the outer lateral surface of the ClC-K2 chloride channel. *Biochem. Biophys. Res. Commun.* **362,** 858–864
45. Gradogna, A., Babini, E., Picollo, A., and Pusch, M. (2010) A regulatory calcium-binding site at the subunit interface of CLC-K kidney chloride channels. *J. Gen. Physiol.* **136,** 311–323